

# Hydrogenation of cyclohexanone on Pt–Sn surface alloys

A. Olivas,<sup>1</sup> Dmitri I. Jerdev, and Bruce E. Koel<sup>\*</sup>

University of Southern California, Department of Chemistry, Los Angeles, CA 90089-0482, USA

Received 21 March 2003; revised 28 July 2003; accepted 30 July 2003

## Abstract

Hydrogenation of cyclohexanone was studied over Pt(111) and two ordered, Pt–Sn alloy surfaces formed by vapor deposition of Sn on the Pt(111) single crystal surface—the  $(2 \times 2)$  Sn/Pt(111) and  $(\sqrt{3} \times \sqrt{3})R30^\circ$  Sn/Pt(111) surface alloys. The influence of alloying Sn, alloy structure, partial pressures of hydrogen and cyclohexanone, and temperature on the activity and selectivity of these model catalysts toward formation of the corresponding alcohol was investigated. All surfaces were characterized before and after catalytic reaction by XPS and LEED to ensure proper alloy formation and stability. The hydrogenation activity at low temperature (325 K) was substantially higher for both Pt–Sn alloy catalysts than that of the Pt(111) surface, with the activity proportional to the amount of Sn in the surface layer. The apparent activation energy for the hydrogenation of cyclohexanone at 325 K was 16.2, 13.4, and 12.4 kcal/mol for Pt(111),  $(2 \times 2)$  Sn/Pt(111) alloy, and  $(\sqrt{3} \times \sqrt{3})R30^\circ$  Sn/Pt(111) alloy, respectively, and the reaction order in  $H_2$  changed from 0.5 on Pt(111) to 1.5 on both alloys. The selectivity over the two Pt–Sn alloys was the same as for Pt(111), but large changes occurred in the products formed as a function of temperature on all three surfaces. Cyclohexanol was the only product detected below 400 K, but cyclohexene and cyclohexane were the sole products at 425 and 500 K, and the  $C_{12}$ -coupling product cyclohexylcyclohexene was formed exclusively at 600 K over all catalysts.

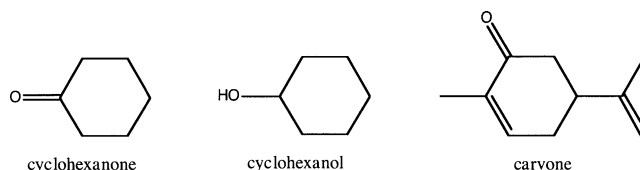
© 2003 Elsevier Inc. All rights reserved.

**Keywords:** Cyclohexanone; Pt; Catalysis; Hydrogenation; Pt–Sn alloy; Alloy catalyst; Cyclohexanol; Bimetallic catalyst

## 1. Introduction

Reflecting their commercial importance, there have been a number of studies aimed at understanding and controlling catalytic reaction selectivity of carbonyl groups, in particular investigations comparing hydrogenation reactions of olefin and carbonyl functional groups [1,2]. However, investigations of the hydrogenation of cyclic hydrocarbons containing carbonyl groups over transition-metal catalysts are scarce despite their importance in catalysis. Cyclohexanone, a monocyclic ketone (Scheme 1) is of great importance as a stable intermediate in hydrodeoxygenation (HDO) reaction sequences [3]. For instance, cyclohexanone is an intermediate in the production from cyclohexanol (Scheme 1) of  $\epsilon$ -caprolactam that is used in the manufacturing of nylon-6 and polyamide resins [4].

Catalytic hydrogenation of cyclohexanone has been studied over a Pt/SiO<sub>2</sub> catalyst [5] in the liquid phase and on



Scheme 1.

Pt/HZSM5 [6] in the gas phase. It was assumed that metallic sites were responsible for hydrogenation reactions and for dehydrogenation into aromatics. Results from the hydrogenation of the unsaturated ketone carvone (Scheme 1) on Pt/Al<sub>2</sub>O<sub>3</sub> and Pt–Sn/Al<sub>2</sub>O<sub>3</sub> indicate that increasing the amount of Sn added to a Pt catalyst favors the formation of unsaturated ketones [7]. Numerous investigations have been carried out to establish the hydrogenation mechanism of ketones in the liquid phase over supported metal or metal sulfide catalysts [9], but to our knowledge, there are no kinetic data available on such reactions over unsupported bimetallic catalysts.

In related catalytic studies of cyclohexene hydrogenation on a Pt(111) single-crystal model catalyst [8], hydrogenation was the only detectable reaction pathway over the tempera-

<sup>\*</sup> Corresponding author.

E-mail address: [koel@usc.edu](mailto:koel@usc.edu) (B.E. Koel).

<sup>1</sup> Permanent address: Centro de Ciencias de la Materia Condensada, UNAM, Ensenada BC, México.

ture range between 300 and 390 K (e.g., no dehydrogenation, cracking, or coupling products were observed). If the surface temperature was increased beyond 390 K, the hydrogenation rate decreased and the onset of a new reaction, dehydrogenation, was also observed.

In this report, we describe studies of cyclohexanone as a model compound for understanding the gas-phase hydrogenation of cyclic ketones over metallic sites on bimetallic Pt–Sn catalysts as probed by experiments using the Pt(111) surface and two ordered Sn–Pt(111) surface alloys as model catalysts.

## 2. Experimental methods

The experiments were performed in an ultrahigh vacuum (UHV) stainless-steel chamber with a base pressure of  $1 \times 10^{-10}$  Torr, pumped with an ion pump (240 L/s) and Cryo-Plex 8 cryogenic pump (1500 L/s), that is coupled directly to a high-pressure reaction chamber via an attendant sample-transfer rod [13]. The UHV chamber was equipped with a spherical capacitor analyzer (SCA) used for Auger electron (AES) and X-ray photoelectron spectroscopy (XPS) [10], and low-energy ion scattering (LEIS), low-energy electron diffraction (LEED) optics, quadrupole mass spectrometer (QMS), and several gas dosers and metal deposition sources. The gas from the reaction cell was analyzed by a HP Model 5890 Series II gas chromatograph (GC) with a capillary column.

The Pt crystal was polished on both sides along the (111) crystal plane. The sample was spot-welded between two tungsten wires (0.8-mm diameter) that connected to Cu feedthrough posts and could be resistively heated from 300 to 1200 K. A chromel–alumel thermocouple was spot-welded directly to the side of the crystal. The clean Pt(111) surface was prepared by Ar<sup>+</sup>-ion sputtering at room temperature for 1 h and annealing at 1000 K in  $1 \times 10^{-7}$  Torr O<sub>2</sub> for 5 min. Sample cleanliness was checked with AES and LEED.

The two Pt–Sn surface alloys were prepared following the procedure described by Paffet and Windham [9]. Sn was evaporated onto the Pt(111) surface at 300 K in UHV and then the sample was annealed at 1000 K for 10 s. LEED and XPS were employed to ensure that the proper alloy was formed on both sides of the crystal. LEED showed the same pattern and the Pt(4f)/Sn(3d) XPS ratio was within 10% on both sides in all cases.

Cyclohexanone (99.5% purity, Aldrich Corp.) was purified by fractional vacuum distillation. Hydrogen (Matheson, 99.9999%) was used as purchased. The reaction mixture was analyzed by using the GC before being introduced into the reaction cell. The analysis showed > 99.99 mass% cyclohexanone, with the rest (< 0.01 mass%) as cyclohexane. We also performed blank experiments before reactions to ensure zero catalytic activity in the absence of the single-crystal catalyst.

Results from our catalytic studies are described by selectivity ( $S_i$ ), conversion ( $C$ ), and turnover frequency (TOF). The calculations done to obtain these values are the same as those in a previous report [13]. The selectivity was calculated for a conversion of less than 10 mol% (unless stated otherwise) in order to reduce the influence of poisoning and secondary products.

Selectivity ( $S_i$ ) toward a given product can be defined by

$$S_i = \frac{n_i}{\sum_i n_i}, \quad (1)$$

where  $n_i$  is the number of moles of a given product. Conversion ( $C$ ) can be defined as

$$C = 1 - \frac{n_{\text{final}}}{n_{\text{initial}}}, \quad (2)$$

where  $n_{\text{initial}}$  and  $n_{\text{final}}$  are the initial and final number of moles of the cyclohexanone reactant.

Activity is expressed as a turnover frequency (TOF) which can be defined as the number of cyclohexanone molecules transformed per surface atom per second. This was determined from initial activities, calculated from the initial slope of plots of the amount of cyclohexanone converted versus time as given by

$$\text{TOF} = \frac{V_R \times N_A \times P_{\text{initial}}}{R \times T \times t \times \Theta_{\text{Pt}} \times S_{\text{Pt}}} \left( 1 - \frac{P_{\text{final}}}{P_{\text{initial}}} \right), \quad (3)$$

where  $V_R$  is the reactor volume ( $3.84 \times 10^{-4}$  m<sup>3</sup>),  $P_{\text{initial}}$  and  $P_{\text{final}}$  are the initial and final pressures of cyclohexanone in the reaction mixture,  $N_A$  is Avogadro's number,  $R$  is the gas constant,  $T$  is the temperature of the reaction mixture (325 K),  $\Theta_{\text{Pt}}$  is the Pt-atom density at the Pt(111) surface ( $1.505 \times 10^{15}$  atoms/cm<sup>2</sup>),  $t$  is the reaction time (s), and  $S$  is the total surface area of the crystal (1.7 cm<sup>2</sup>). No corrections were done for decreasing the surface Pt-atom concentration in the alloys. We note that Eq. (3) is the same as Eq. (3) in Ref. [13], which is obtained by substituting the mole fraction of cyclohexanone  $X_{\text{CHO}}$  for the cyclohexanone partial pressures in the reaction mixture ( $X_{\text{CHO}}$  was misdefined in Ref. [13] as mole percent, however). Eq. (3) is only valid if the number of moles of product produced is equal to the number of moles of the cyclohexanone reactant consumed for each of the products formed in the reaction.

## 3. Results

Catalytic hydrogenation of cyclohexanone was carried out over a temperature range of 325–600 K. The temperature of the reactor walls was kept at 325 K in order to minimize possible condensation of reactant and product gases.

The conversion of cyclohexanone over Pt(111) and two ordered Sn/Pt(111) surface alloys is shown in Figs. 1–3 as a function of reaction time for different catalyst temperatures. Over Pt(111) at the lowest temperature investigated of 325 K, it took 500 s to reach 10% cyclohexanone conversion

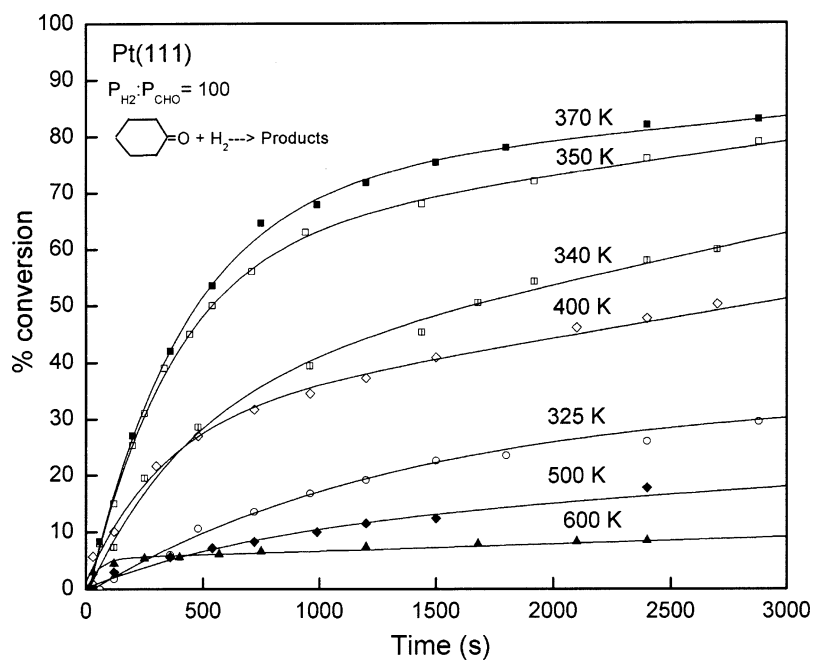
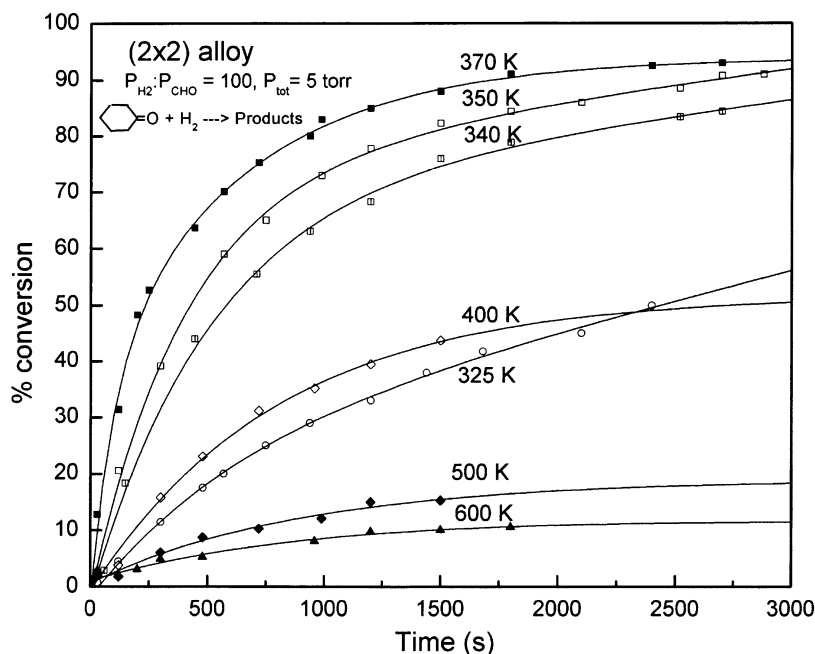


Fig. 1. Catalytic hydrogenation of cyclohexanone over Pt(111).

Fig. 2. Catalytic hydrogenation of cyclohexanone over a (2 × 2) Sn/Pt(111) alloy with Θ<sub>Sn</sub> = 0.25.

as shown in Fig. 1. This level of conversion was reached after only 100 s at catalyst temperatures of 350–400 K. The conversion rapidly increased upon contact with the catalyst, and there was no indication of an induction or activation period for the reaction at these temperatures. Conversion after 3600 s (60 min) reached 80, 85, and 55% for catalyst temperatures of 350, 370, and 400 K, respectively. The curves shown in Fig. 1 exhibit exponential shapes commonly observed in catalytic transformations for similar heterogeneous systems using a batch reactor.

The (2 × 2) Sn/Pt(111) alloy with Θ<sub>Sn</sub> = 0.25 was much more active than Pt(111) at low temperatures, as shown in Fig. 2. At 325 K, 10% conversion was reached in only 200 s. Almost the same behavior was observed when using the (√3 × √3)R30° Sn/Pt(111) alloy as a catalyst, as shown in Fig. 3. At 350 and 370 K the initial rates were nearly the same; however, the rate at 325 K was faster and the rate at higher temperatures was slower than that on the (2 × 2) alloy.

The selectivity data as a function of temperature were similar for all three of these catalysts. Specifically, results for

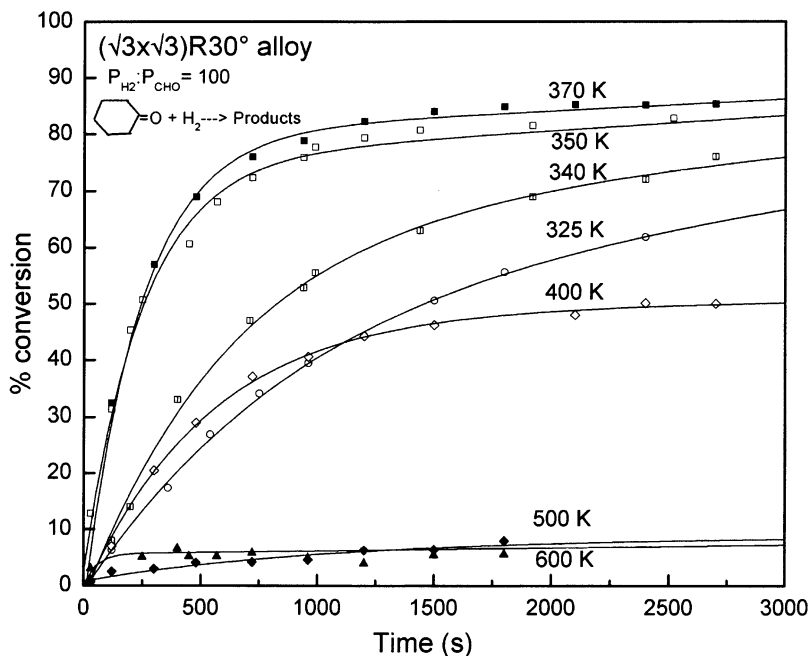


Fig. 3. Catalytic hydrogenation of cyclohexanone over a  $(\sqrt{3} \times \sqrt{3})R30^\circ$  Sn/Pt(111) alloy with  $\Theta_{\text{Sn}} = 0.33$ .

Pt(111) at low (< 20%) conversion are presented in Fig. 4. Temperature has a strong effect on the reaction selectivity. The main product of the hydrogenation of cyclohexanone over all of the catalysts was cyclohexanol in the temperature range of 325–400 K. At 425–500 K, the main products were cyclohexene and cyclohexane, with only a trace of cyclohexanol. At 600 K, the reaction was essentially 100% selective for cyclohexylcyclohexene. No benzene or phenol was detected under any of these reaction conditions.

The influence of temperature on the initial reaction rate, as monitored at < 10% conversion, was determined over a wide range of catalyst temperatures at a fixed pressure ratio of cyclohexanone (CHO) to  $\text{H}_2$  of 1:100 with  $P_{\text{total}} = 5$  Torr as shown in Fig. 5. Because only hydrogenation to form cyclohexanol occurs in the low temperature range near 325 K, an apparent activation energy,  $E_a(\text{app})$ , for the hydrogenation of the C=O functional group can be calculated by considering the lowest temperature data (350, 340, and

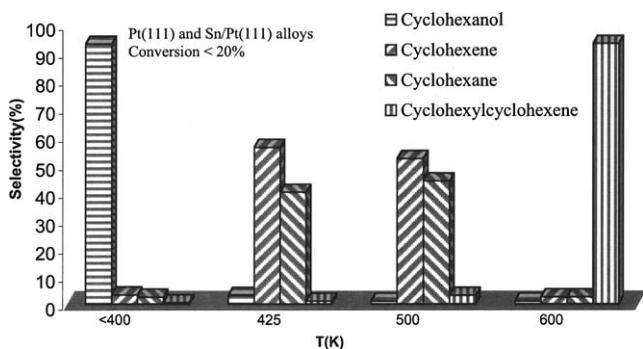


Fig. 4. Selectivities of cyclohexanone hydrogenation (< 20% conversion) as a function of the reaction temperature.

325 K) shown in Fig. 5. Values of  $E_a(\text{app}) = 16.2, 13.4$ , and  $12.4$  kcal/mol at < 10% conversion were determined for Pt(111) and the  $(2 \times 2)$  and  $(\sqrt{3} \times \sqrt{3})R30^\circ$  surface alloys, respectively. These values are provided in Table 1. Arrhenius behavior of the hydrogenation rate from 325 to 350 K over Pt(111) and the  $(2 \times 2)$  alloy implies that the number of surface active sites does not change in any significant manner over this range of temperature. This factor may be influencing the data on the  $(\sqrt{3} \times \sqrt{3})R30^\circ$  alloy, however. At these low temperatures, alloying and increasing the amount of Sn at the Pt–Sn surface increases the catalytic activity and decreases the apparent activation energy. As a

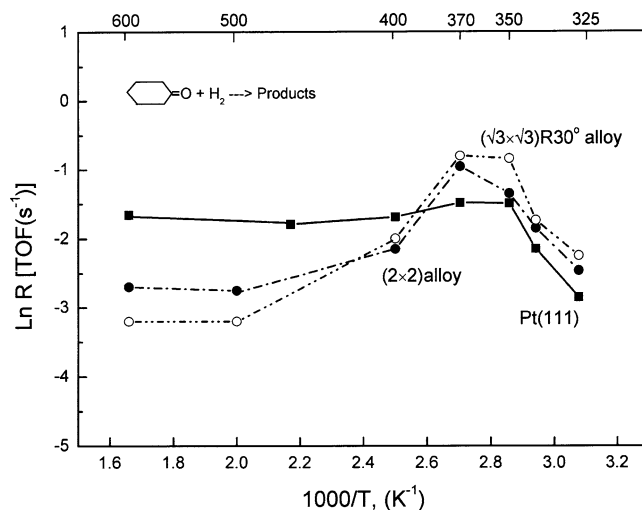


Fig. 5. Arrhenius plots for Pt(111) (■) and the  $(2 \times 2)$  (●) and  $(\sqrt{3} \times \sqrt{3})R30^\circ$  Sn/Pt(111) surface alloys.  $P_{\text{H}_2} = 5$  Torr and  $P_{\text{cyclohexanone}} = 5 \times 10^{-2}$  Torr.

Table 1  
Hydrogenation of cyclohexanone over Pt and Sn/Pt catalysts<sup>a</sup>

Catalyst	Sn coverage (ML)	$E_a$ (app) <sup>b</sup> (kcal/mol)	Overall hydrogenation activity, TOF (s <sup>-1</sup> )
Pt(111)	0	16.2	0.064
(2 × 2) Sn/Pt(111) alloy	0.25	13.4	0.085
( $\sqrt{3} \times \sqrt{3}$ )R30° Sn/Pt(111) alloy	0.33	12.4	0.096

<sup>a</sup>  $P_{H_2}:P_{CHO} = 100$ ,  $P_{total} = 5$  Torr, and  $T_{gas} = 325$  K.

<sup>b</sup> Evaluated by using data at 350, 340, and 325 K. The uncertainty is estimated roughly to be  $\leq 1$  kcal/mol.

point of comparison, the apparent activation energy for ethylene hydrogenation over Pt(111) at 300–370 K has been reported to be 10.8 kcal/mol [21].

At 400 and 500 K, all of the catalysts favor dehydration of cyclohexanol to form cyclohexene and cyclohexane. The measured initial reaction rate drops sharply for both alloy catalysts between 370 and 400 K. The dehydration reaction rate decreases as the temperature is raised above 400 K, and at 600 K, a new compound, cyclohexylcyclohexene, is produced with high selectivity.

The reaction kinetics were also measured as a function of partial pressures of hydrogen and cyclohexanone. Data for the dependence of the rate of cyclohexanone conversion on hydrogen pressure over all three catalysts at 370 K is given in Fig. 6. The rate exhibits a reaction order of 0.5 in hydrogen pressure for Pt(111) and 1.5 for both alloys. The rate for all three catalysts shows a negative reaction order in the reactant pressure. Over Pt(111), the reaction order in cyclohexanone is  $-0.6$  and is  $-0.9$  over both alloys, as shown in Fig. 7.

Fig. 8 summarizes some of our data, replotting to explicitly show the influence of the Sn content on the activity for cyclohexanone conversion over these catalysts at different reaction temperatures. When Sn was alloyed with Pt, the ac-

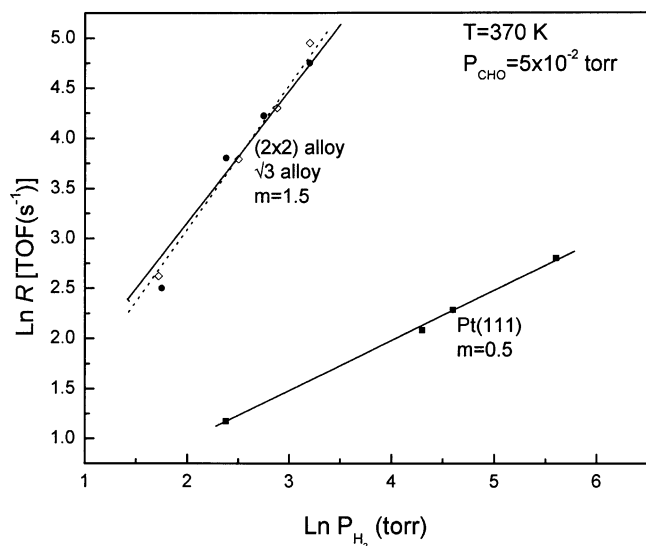


Fig. 6. Effect of the hydrogen pressure on the catalytic hydrogenation of cyclohexanone over Pt(111) and Sn/Pt(111) surface alloys.

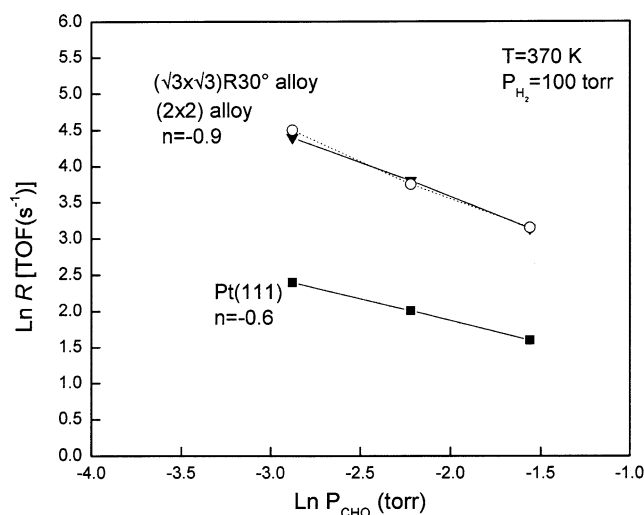


Fig. 7. Effect of the cyclohexanone pressure on the catalytic hydrogenation of cyclohexanone over Pt(111) and Sn/Pt(111) surface alloys.

tivity of the catalyst at 325 to 370 K increased in proportion to the amount of Sn in the surface layer. The highest activity that we measured was for the ( $\sqrt{3} \times \sqrt{3}$ )R30° at 370 K. At catalyst temperatures of 400 K or higher, all of the catalysts have a lower rate and increasing the amount of Sn in the alloy surface decreased the conversion rate. One imagines that at some temperature between 370 and 400 K there is no effect of alloying Sn on the rate.

#### 4. Discussion

The selectivity is mainly to cyclohexanol in the 325–400 K temperature range for all catalysts in the hydrogenation reaction of cyclohexanone. It was reported for cyclo-

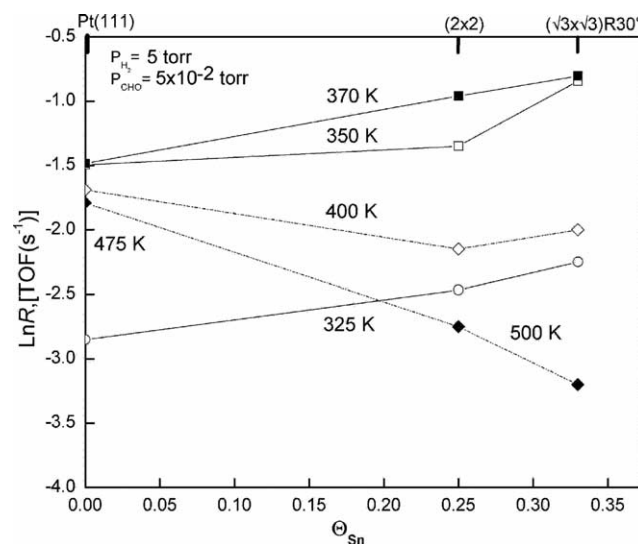


Fig. 8. Reaction rate for catalytic hydrogenation of cyclohexanone over Pt(111) and Sn/Pt(111) surface alloys as a function of the surface Sn concentration.

hexene hydrogenation on Pt(111) [8] that only cyclohexane was formed in the reaction at the 300–400 K temperature range. Alloyed Sn does not appreciably modify the Pt(111) selectivity. It has an effect on the reaction rate where, at low temperature, increasing the amount of tin increases the reaction rate. This increase in rate is attributed to a favorable modification of the nature of the active metallic sites.

Our results on Pt(111) selectivity agree with those obtained on Pt/SiO<sub>2</sub> catalysts (5% by weight Pt on silica of grain size 0.05–0.125 mm) in the pressure range 0.1 to 150 bar and room temperature [5], and also agree with the results of Alvarez et al. [6]. They reported 6 groups of products for cyclohexanone hydrogenation on PtHZSMS catalysts (0.05 and 0.2 wt% Pt) at 473 K, under atmospheric pressure in a flow reactor with a H<sub>2</sub>/CHO molar ratio of 3. In our case, for the range 425 to 500 K, cyclohexanol, cyclohexene, cyclohexane, and cyclohexylcyclohexene are among those products reported by Alvarez et al., but we did not observe the variety of products that they reported. We can say that for 425–500 K dehydration proceeds prior to ring hydrogenation or dehydrogenation in the reaction mechanism. The cyclohexylcyclohexene formed selectively at 600 K over our catalysts could result from the dimerization of cyclohexene [6] or dehydration of cyclohexylcyclohexanone [11].

To our knowledge this is the first report of catalytic cyclohexanone hydrogenation on a clean Pt single crystal surface or unsupported Pt–Sn alloys, specifically Pt(111) and two well-characterized Sn/Pt(111) alloys. Thus, a reaction scheme can be presented that is not influenced by participation of an oxide support or oxidized Sn species. The products of cyclohexanone hydrogenation result from the following steps on metallic sites:

- 325–400 K Hydrogenation of cyclohexanone;
- 400–500 K Dehydration of cyclohexanol followed by hydrogenation or dehydrogenation of the cyclohexyl ring;
- 600 K Ring coupling and formation of bicyclic hydrocarbons.

In the prior literature, there are no values reported for apparent activation energies,  $E_a(\text{app})$ , of gas-phase hydrogenation of cyclohexanone over platinum-based catalysts. We found that  $E_a(\text{app})$  for cyclohexanone hydrogenation decreased as the Sn/Pt atomic ratio increased. This qualitatively accounts for the increase in the reaction rates. A qualitatively similar trend was observed for crotonaldehyde (CH<sub>2</sub>=CHCH<sub>2</sub>CHO) hydrogenation on supported and unsupported Pt–Sn bimetallic catalysts [12,13].

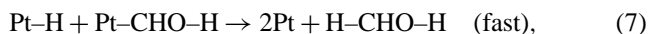
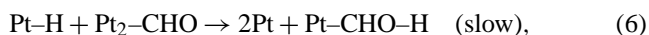
The steep decrease in the reaction rate over the alloys from 370 to 400 K can be attributed to a change in reaction mechanism and the rate-determining step that occurs when the product distribution changes from cyclohexanol to cyclohexene and cyclohexane. The C–O bond cleavage that occurs in dehydration is expected to proceed only with a large activation energy barrier on the alloys. However, this

decrease in activity and also the non-Arrhenius behavior already at 370 K on Pt(111) could be attributed to deactivation due to the buildup of hydrocarbon intermediates or carbonaceous deposits [14]. We observed larger amounts of carbon on all three surfaces following high-pressure reaction at 400 K compared to that at lower temperatures.

The reaction order in hydrogen of 0.5 found for Pt(111) is consistent with a proposal that H<sub>2</sub> is weakly and dissociatively adsorbed on the surface in a Langmuir–Hinshelwood mechanism [15]. The negative reaction order in cyclohexanone determined here is also consistent with strong ketone adsorption on the surface of the metal catalyst. Cyclohexanone temperature-programmed desorption (TPD) studies reported elsewhere [16,17] show that cyclohexanone is strongly bound, and even partially irreversibly adsorbed at low coverages under UHV conditions, on Pt and Pt–Sn alloys.

These reaction orders are comparable to those observed for liquid-phase hydrogenation of cyclohexanone over Pt/SiO<sub>2</sub> [5]. In the case of 2-cyclohexenone hydrogenation over Pt/SiO<sub>2</sub>, the order with respect to the ketone was  $-1.4$  [18]. Negative orders with respect to the ketone were also reported for hydrogenation reactions of 1,4-cyclohexanedione and acetophenone [19,20].

According to a Langmuir–Hinshelwood mechanism, and assuming that hydrogen and the ketone are both adsorbed on (energetically) equivalent Pt sites, a simplified mechanism can be proposed for hydrogenation of cyclohexanone to produce cyclohexanol at 325–370 K as follows:



where CHO denotes C<sub>6</sub>H<sub>10</sub>O (cyclohexanone) and H-CHO-H denotes C<sub>6</sub>H<sub>12</sub>O (cyclohexanol).

In Eqs. (4) and (5), hydrogen and CHO compete for Pt sites. In Eq. (5), CHO is assumed to chemisorb in a di- $\sigma$  manner with a stoichiometry of 2 Pt sites per molecule. Hydrogenation in either Eqs. (6) or (7) is assumed to be the rate-determining step because we expect cyclohexanol desorption to be fast at 300 K [16]. In our derivation, we assume Eq. (6) to be the rate-determining step. An inhibiting effect often observed for CHO can be explained by a stronger interaction of CHO than hydrogen with Pt.

The overall reaction rate is determined by Eq. (6) and can be expressed by

$$r_{\text{CHO}} = k\Theta_{\text{CHO}}\Theta_{\text{H}}, \quad (8)$$

where,  $r_{\text{CHO}}$  is the rate of disappearance of CHO,  $k$  is an Arrhenious rate constant, and  $\Theta_{\text{CHO}}$  and  $\Theta_{\text{H}}$  are the adsorbed cyclohexanone and hydrogen adatom coverages, respectively, and CHO and H adsorb on neighboring sites with a probability proportional to the product of coverages  $\Theta_{\text{CHO}} \cdot \Theta_{\text{H}}$ .

An equilibrium constant  $K_{H_2}$  for dissociative  $H_2$  chemisorption as given in Eq. (4) can be written as

$$\frac{\Theta_H}{\Theta_{Pt} P_{H_2}^{1/2}} = K_{H_2}^{1/2}, \quad (9)$$

where  $\Theta_{Pt}$  is the Pt surface available (unoccupied) for adsorption, and  $P_{H_2}$  is the  $H_2$  partial pressure.

An equilibrium constant  $K_{CHO}$  for chemisorption in Eq. (5) can be written as

$$\frac{\Theta_{CHO}}{\Theta_{Pt}^2 P_{CHO}} = K_{CHO}. \quad (10)$$

Because

$$\Theta_{Pt} = (1 - \Theta_H - \Theta_{CHO}) \quad (11)$$

in cases of fast desorption of products, we can write a system of two simultaneous equations as

$$\Theta_H = K_{H_2}^{1/2} P_{H_2}^{1/2} (1 - \Theta_H - \Theta_{CHO}), \quad (12)$$

$$\Theta_{CHO} = K_{CHO} P_{CHO} (1 - \Theta_H - \Theta_{CHO})^2 \quad (13)$$

that must be solved simultaneously to find  $\Theta_H$  and  $\Theta_{CHO}$  in terms of the measured partial pressures. Solving this set of equations by eliminating  $\Theta_{CHO}$  using

$$\Theta_{CHO} = \left( \frac{K_{CHO} P_{CHO}}{K_{H_2} P_{H_2}} \right) \Theta_H^2 \quad (14)$$

leads to a quadratic equation in  $\Theta_H$ . Only one solution to the quadratic expression that results is physically meaningful to allow for  $\Theta_H > 0$ , and we obtain

$$\Theta_H = \frac{1}{2} \left[ - \left( \frac{\frac{K_{CHO} P_{CHO}}{K_{H_2} P_{H_2}} + \frac{K_{CHO} P_{CHO}}{K_{H_2}^{1/2} P_{H_2}^{1/2}}}{\frac{K_{CHO}^2 P_{CHO}^2}{K_{H_2}^{3/2} P_{H_2}^{3/2}}} \right) + \sqrt{\left( \frac{\frac{K_{CHO} P_{CHO}}{K_{H_2} P_{H_2}} + \frac{K_{CHO} P_{CHO}}{K_{H_2}^{1/2} P_{H_2}^{1/2}}}{\frac{K_{CHO}^2 P_{CHO}^2}{K_{H_2}^{3/2} P_{H_2}^{3/2}}} \right)^2 + \frac{4 K_{H_2} P_{H_2}}{K_{CHO} P_{CHO}}} \right]. \quad (15)$$

Eq. (14) can be used to rewrite Eq. (8) in terms of only  $\Theta_H$

$$r_{CHO} = k \left( \frac{K_{CHO} P_{CHO}}{K_{H_2} P_{H_2}} \right) \Theta_H^3. \quad (16)$$

The complicated expression that gives  $\Theta_H$  in Eq. (15) can be simplified for our reaction conditions assuming that

$$K_{CHO} P_{CHO} \ll K_{H_2} P_{H_2} \quad (17)$$

to give

$$\Theta_H = \left( \frac{K_{H_2} P_{H_2}}{K_{CHO} P_{CHO}} \right)^{1/2}. \quad (18)$$

This expression can be substituted into Eq. (16) to give

$$r_{CHO} = k' P_{CHO}^{-1/2} P_{H_2}^{1/2}, \quad (19)$$

where  $k' = (k K_{H_2}^{1/2} / K_{CHO}^{1/2})$ . This expression, Eq. (19), is in good agreement with our experimental results for the Pt(111) surface given by

$$r_{CHO} = k P_{CHO}^{-0.6} P_{H_2}^{0.5}. \quad (20)$$

Experimentally, we tried to prevent excessive carbon residue formation by using a high hydrogen/hydrocarbon ratio. This condition also introduces the so-called “quasi-zero” order with respect to hydrogen, because the hydrogen concentration in the reaction mixture does not change significantly during the reaction run. However, varying the hydrogen pressure in the mixture must result in the correct order of the reaction in  $H_2$ , independent of the above reasoning, also, the order in cyclohexanone indicates that its inhibiting effect diminishes in the experimental conditions used.

In the case of the two Sn/Pt(111) alloy catalysts, our experimental results give

$$r_{CHO} = k P_{CHO}^{-0.9} P_{H_2}^{1.5}. \quad (21)$$

This rate equation differs with respect to that for Pt(111) by a decrease of  $-0.3$  in the reaction order in cyclohexanone and an increase of  $1.0$  in the reaction order in  $H_2$ . The change in hydrogen reaction order is consistent with previous UHV studies of  $H_2$  adsorption on the Pt–Sn alloys [22] where it was shown that the barrier for  $H_2$  dissociative adsorption increases on these surfaces compared to Pt(111). In addition it is also known that hydrocarbon adsorption is also weaker on the Pt–Sn surface alloys [23–25]. On the alloys, the overall reaction rate, instead of being determined mostly by the reaction in Eq. (6), is distributed more equally among steps in Eqs. (4)–(6) making the rate more sensitive to the pressures of the reactants. This would increase the importance of the competition for adsorption sites in the overall reaction rate compared to that on Pt(111) and induce a change in the absolute values of the reaction orders from  $0.5$  to  $1.5$  for hydrogen and from  $-0.6$  to  $-0.9$  for cyclohexanone.

As a final point of interest, the kinetic data for cyclohexanone hydrogenation over the Sn/Pt(111) alloy catalysts can be compared with extensive studies of ethylene hydrogenation over Pt(111) [21] where the reaction orders were  $1.31$  and  $-0.6$  in  $H_2$  and ethylene, respectively. These results more closely agree with our results on cyclohexanone over the two Pt–Sn alloys than our results on Pt(111).

## 5. Conclusion

Using two unsupported, well-defined Sn/Pt(111) model catalysts for the gas-phase hydrogenation of cyclohexanone, we report activities and selectivities compared to unsupported Pt(111) catalysts. Alloying tin to platinum and increasing the amount of alloyed tin enhances the overall catalytic activity toward the corresponding alcohol, cyclohexanol, at low temperatures, specifically  $325$  K. There is no appreciable change in selectivity between Pt(111) and the two Sn/Pt(111) alloys.

## Acknowledgments

This work was supported by the US Department of Energy, Office of Basic Energy Sciences, Chemical Sciences Division. A. Olivas thanks Conacyt for providing a scholarship.

## References

- [1] T.B.L.W. Marinelli, J.H. Vleeming, V. Ponc, D. Wang, D.G. Blackmond, D. Arntz, G. Jannes, K. Kunimori, C.H. Rochester, *Stud. Surf. Sci. Catal. B* 75 (1993) 1211.
- [2] E. Ronzon, G. Del Angel, *J. Mol. Catal.* 148 (1999) 105.
- [3] H. Schulz, N.M. Rahman, M. Breyse, P. Tetenyi, D. Kallo, H.J. Lovink, M.R. Deagudelo, *Stud. Surf. Sci. Catal. A* 75 (1993) 585.
- [4] G. Neri, A.M. Visco, A. Donato, C. Milone, M. Malentacchi, G. Gu-bitosa, *Appl. Catal. A* 110 (1994) 49.
- [5] P. Geneste, M. Bonnet, M. Rodriguez, *J. Catal.* 57 (1979) 147.
- [6] F. Alvarez, P. Magnoux, F. Ramoa Ribeiro, M. Guisnet, *J. Mol. Catal.* 92 (1994) 67.
- [7] G.C. Torres, S.D. Ledezma, E.L. Jablonski, S.R. de Miguel, O.A. Scelza, *Catal. Today* 48 (1999) 65.
- [8] X. Su, K.Y. Kung, J. Lahtinen, Y.R. Shen, G.A. Somorjai, *J. Mol. Catal. A* 141 (1999) 9.
- [9] M.T. Paffet, R.G. Windham, *Surf. Sci.* 34 (1989) 28.
- [10] J.F. Moulder, W.F. Stickle, P.E. Sobol, K.D. Bomben, *Handbook of X-Ray Photoelectron Spectroscopy*, Perkin-Elmer, Eden Prairie, MN, 1992.
- [11] A.I. Silva, F. Alvarez, F.R. Ribeiro, M. Guisnet, *Catal. Today* 60 (2000) 311.
- [12] F. Coloma, A. Sepúlveda-Escribano, J.L.G. Fierro, F. Rodriguez-Reinoso, *Appl. Catal. A* 136 (1996) 231.
- [13] D.I. Jerdev, A. Olivas, B.E. Koel, *J. Catal.* 205 (2002) 278.
- [14] C.M. Pradier, E. Margot, Y. Berthier, J. Oudar, *Appl. Catal. A* 43 (1988) 77.
- [15] R.J. Masel, *Principles of Adsorption and Reaction on Solid Surfaces*, Wiley, New York, 1996.
- [16] A. Olivas, A. Kim, J. Koel, E. Bruce, *Surf. Sci.*, submitted for publication.
- [17] S. Zhuang, X. Wang, X. Wei, Y. Wang, S. Ren, R. Zhai, *Surf. Sci.* 376 (1997) L429.
- [18] P. Geneste, M. Bonnet, C. Frouin, *J. Catal.* 90 (1984) 147.
- [19] M. Bonnet, P. Geneste, M. Rodriguez, *J. Org. Chem.* 45 (1980) 40.
- [20] P. Geneste, Y. Lozano, C. R. Acad. Sci., Ser. C 280 (1975) 1137.
- [21] F. Zaera, G.A. Somorjai, *J. Am. Chem. Soc.* 107 (1985) 5910.
- [22] M.T. Paffett, S.C. Gebhard, R.G. Windham, B.E. Koel, *J. Phys. Chem.* 94 (1990) 6831.
- [23] M.R. Voss, H. Busse, B.E. Koel, *Surf. Sci.* 414 (1998) 330.
- [24] C. Xu, Y.-L. Tsai, B.E. Koel, *Surf. Sci.* 304 (1994) 249.
- [25] Y.-L. Tsai, C. Xu, B.E. Koel, *Surf. Sci.* 385 (1997) 37.